Single-cell RNA sequencing identifies senescent cerebromicrovascular endothelial cells in the aged mouse brain

Tamas Kiss · Ádám Nyúl-Tóth · Priya Balasubramanian · Stefano Tarantini ·
Chetan Ahire · Jordan DelFavero · Andriy Yabluchanskiy · Tamas Csipo · Eszter Farkas ·
Graham Wiley · Lori Garman · Anna Csiszar · Zoltan Ungvari

Abstract Age-related phenotypic changes of cerebromicrovascular endothelial cells lead to dysregulation of cerebral blood flow and blood-brain barrier disruption, promoting the pathogenesis of vascular cognitive impairment (VCI). In recent years, endothelial cell senescence has emerged as a potential mechanism contributing to microvascular pathologies opening the avenue to the therapeutic exploitation of senolytic drugs in preclinical studies. However, difficulties with the detection of senescent endothelial cells in wild type mouse models of aging hinder the assessment of the efficiency of senolytic treatments. To detect senescent endothelial cells in the aging mouse brain, we analyzed 4233 cells in fractions enriched for cerebromicrovascular endothelial cells and other cells

Tamas Kiss, Ádám Nyúl-Tóth, Priya Balasubramanian and Stefano Tarantini contributed equally to this work.

T. Kiss · Á. Nyúl-Tóth · P. Balasubramanian · S. Tarantini ·
C. Ahire · J. DelFavero · A. Yabluchanskiy · T. Csipo ·
A. Csiszar (✉) · Z. Ungvari
Department of Biochemistry and Molecular Biology, Reynolds Oklahoma Center on Aging/Center for Geroscience and Healthy Brain Aging, Vascular Cognitive Impairment and Neurodegeneration Program, University of Oklahoma Health Sciences Center, 975 NE 10th Street, Oklahoma City, OK 73104, USA
e-mail: anna-csiszar@ouhsc.edu

T. Kiss · E. Farkas · A. Csiszar · Z. Ungvari
Department of Medical Physics and Informatics, International Training Program in Geroscience, Theoretical Medicine Doctoral School, University of Szeged, Szeged, Hungary

Á. Nyúl-Tóth
Biological Research Centre, Institute of Biophysics, Szeged, Hungary

S. Tarantini · T. Csipo · Z. Ungvari
Department of Health Promotion Sciences, College of Public Health, University of Oklahoma Health Sciences Center, Oklahoma City, OK, USA

S. Tarantini · A. Yabluchanskiy · Z. Ungvari
Department of Public Health, International Training Program in Geroscience, Doctoral School of Basic and Translational Medicine, Semmelweis University, Budapest, Hungary

T. Csipo
Department of Cardiology, International Training Program in Geroscience, Division of Clinical Physiology, Faculty of Medicine, University of Debrecen, Debrecen, Hungary

G. Wiley · L. Garman
Genes & Human Disease Research Program, Oklahoma Medical Research Foundation, Oklahoma City, OK, USA

A. Csiszar · Z. Ungvari
The Peggy and Charles Stephenson Cancer Center, University of Oklahoma Health Sciences Center, Oklahoma City, OK 73104, USA

associated with the neurovascular unit obtained from young (3-month-old) and aged (28-month-old) C57BL/6 mice. We define 13 transcriptomic cell types by deep, single-cell RNA sequencing. We match transcriptomic signatures of cellular senescence to endothelial cells identified on the basis of their gene expression profile. Our study demonstrates that with advanced aging, there is an increased ratio of senescent endothelial cells (~ 10%) in the mouse cerebral microcirculation. We propose that our single-cell RNA sequencing–based method can be adapted to study the effect of aging on senescence in various brain cell types as well as to evaluate the efficiency of various senolytic regimens in multiple tissues.

Introduction

The human brain is supplied by 600 km of capillaries consisting of 5×10^9 cerebromicrovascular endothelial cells (Ungvari et al. 2018a; Tarantini et al. 2017a). Healthy function of cerebromicrovascular endothelial cells is critical for adequate oxygen and nutrient delivery to neurons; clearance of toxic metabolites; prevention of amyloid plaque formation; maintenance of the blood-brain barrier; transendothelial transport of substances, hormones, and metabolites; controlling the structural remodeling of the cerebral microcirculation (including angiogenesis, vessel regression, adaptation to hypertension (Ungvari et al. 2018a; Csiszar et al. 2017; Tarantini et al. 2016; Tucsek et al. 2014a; Warrington et al. 2013; Ungvari et al. 2013a; Ungvari et al. 2017a; Tarantini et al. 2017b; Toth et al. 2015)); deposition of the extracellular matrix and synthesis of the glycocalyx; regulation of adhesion and extravasation of inflammatory circulating cells that participate in central nervous system immune surveillance (Stanimirovic and Friedman 2012); regulation of homing of stem cells; maintenance of the perivascular cellular microenvironment; and regulation of the neurogenic niches. There is strong evidence that aging-induced dysregulation of microvascular endothelial function and phenotype critically contributes to the pathogenesis of both vascular cognitive impairment (VCI) and Alzheimer's disease (AD) (Tarantini et al. 2017a; Csiszar et al. 2017; Csipo et al. 2018; Csipo et al. 2019a; Csipo et al. 2019b; Csiszar et al. 2019; Farias Quipildor et al. 2019; Fulop et al. 2019a; Fulop et al. 2018; Kiss et al. 2019a; Kiss et al.

2019b; Lipecz et al. 2019; Tarantini et al. 2017c; Tarantini et al. 2017d; Tarantini et al. 2019a; Montagne et al. 2017; Sweeney et al. 2018a; Castillo-Carranza et al. 2017; Lin et al. 2013). With age, the phenotype and function of cerebromicrovascular endothelial cells are altered, which fundamentally affects all of the aforementioned physiological processes. Aging decreases capillary density (known as "microvascular rarefaction") (Csiszar et al. 2017; Tarantini et al. 2016; Tucsek et al. 2014a; Ungvari et al. 2013a; Banki et al. 2015; Toth et al. 2017) and impairs cerebromicrovascular endothelial vasodilation and endothelium-mediated neurovascular coupling responses (Petzold and Murthy 2011; Stobart et al. 2013; Wells et al. 2015; Chen et al. 2014), which contribute to a decline in cerebral blood flow and promote cognitive decline. In addition, microvascular endothelial aging also disrupts the blood-brain barrier, which promotes neuroinflammation, exacerbating cognitive decline (Tucsek et al. 2014a; Montagne et al. 2017; Toth et al. 2017; Fulop et al. 2019b; Tarantini et al. 2018; Toth et al. 2013; Toth et al. 2014; Tucsek et al. 2014b; Van Skike et al. 2018; Mackic et al. 1998; Montagne et al. 2015; Sweeney et al. 2018b; Zlokovic 2008). In AD, multifaceted microvascular pathologies (including perivascular amyloid deposition and plaque formation, microvascular inflammation, microhemorrhages, blood-brain barrier disruption, ghost vessel formation) contribute to the genesis and progression of the disease (Tucsek et al. 2014a; Ungvari et al. 2017a; Tarantini et al. 2017c; Sweeney et al. 2018a; Sweeney et al. 2018b; Zlokovic 2008; Brown and Thore 2011; Sen and Hongpaisan 2018; Hase et al. 2020; van Veluw et al. 2019; Freeze et al. 2019; Nielsen et al. 2017; Clark et al. 2017; Cifuentes et al. 2017; Nelson et al. 2017; Bell and Zlokovic 2009; Kisler et al. 2017; Nelson et al. 1862; Sagare et al. 2013).

Oxidative stress and macromolecular damage in aged cells induce a complex stress response termed cellular senescence, which has been shown to cause or exacerbate aging and several age-related pathologies (Baker et al. 2016; Campisi 2013; Justice et al. 2018; Khosla et al. 2018; Kirkland and Tchkonia 2017; Tchkonia and Kirkland 2018; Tchkonia et al. 2013; LeBrasseur et al. 2015; Tchkonia et al. 2010; Campisi 2016; Chinta et al. 2018; Chinta et al. 2014). Importantly, recent evidence suggests that endothelial cells are particularly sensitive to reactive oxygen species (ROS) (Nagyoszi et al. 2015; Wilhelm et al. 2017) and other DNA-damaging stressors (Shi et al. 2007; Silva et al. 2017; Voghel et al. 2007) and that cultured cerebromicrovascular endothelial cells

Table 1 Cell clusters resolved by Louvain clustering

Cell type	Cluster	Top 20 marker genes	Young cell #	Aged cell #
Endothelial cell	1	Cldn5, Ly6c1, Itm2a, Ly6a, Slco1a4, Bsg, Flt1, Pglyrp1, Egfl7, Slc2a1, Id1, Pltp, Id3, Abcg2, Tsc22d1, Ifitm3, Igfbp7, Ramp2, Slc6a6, Crip2	417	599
Microglia	0	Hexb, P2ry12, Selplg, Lgmn, C1qa, Ctss, C1qb, C1qc, Ctsd, Csf1r, Cst3, Trem2, Laptm5, Cx3cr1, Tmem119, Gpr34, Fcer1g, Ctsz, Fcrls, Olfml3	622	485
Microglia	2	Junb, Ier5, Jun, Nfkbia, Jund, Ubc, Cd83, Egr1, Csf1r, Zfp36, Ier2, C1qc, Atf3, Ppp1r15a, Hexb, Ctss, Nfkbiz, C1qb, Rhob, Tmem119	351	196
Microglia	6	Lyz2, Cd52, Cd74, Ms4a7, Apoe, Lilrb4a, Cybb, B2m, Rps28, Rps15a, Cst7, Rpl32, H2-Ab1, Rpl39, Ifi27l2a, Rps13, Wfdc17, Rps27, Lgals3, Rpl37a	49	172
Pericyte	9	Vtn, Atp13a5, Higd1b, Ndufa4l2, Kcnj8, Pdgfrb, Rgs5, Slc6a20a, Art3, P2ry14, Ptn, Cox4i2, Cald1, Slc19a1, Ifitm1, Atp1a2, Abcc9, Rgs4, Tbx3os1, Nbl1	71	32
Smooth muscle cell	8	Acta2, Tagln, Myl9, Myl6, Crip1, Tpm2, Dstn, Myh11, Tpm1, Mustn1, Mylk, Pln, Vim, Flna, Cald1, Sncg, Des, Lmod1, Cnn1, Igfbp7	41	83
Astrocyte	4	Gm3764, Gpr37l1, Bcan, Ntm, Ntsr2, Plpp3, Slc1a3, Atp1a2, F3, Clu, Slc7a10, Slc1a2, Atp1b2, Gja1, Cspg5, Cldn10, Htra1, Gria2, Fgfr3, Pla2g7	166	106
Oligodendrocyte	3	Plp1, Cldn11, Cnp, Cryab, Aplp1, Stmn4, Ptgds, Car2, Mbp, Fth1, Mog, Mag, Gatm, Mal, Ermn, Qdpr, Sept4, Mobp, Opalin, Tubb4a	142	160
Neuron	5	Snhg11, Meg3, Camk2n1, Camk2a, Celf2, Ndrg4, Map 2, Camk2b, Celf4, Atp1b1, Rtn1, Cpe, Pcp4, Pcsk1n, Snap25, Adgrb1, mt-Co1, Shank1, Ttc3, Aldoc	127	98

readily acquire senescent phenotypes in response to DNA damage (Ungvari et al. 2013b; Ungvari et al. 2018b). Recent studies suggest that the endothelial senescence contributes to the genesis of cerebromicrovascular aging phenotypes, including microvascular rarefaction, pro-inflammatory alterations, vasomotor dysfunction, and blood-brain barrier disruption. Upon induction of cellular senescence *in culture*, endothelial cells undergo cell cycle arrest and acquire a senescence-associated secretory phenotype (SASP), characterized by increased secretion of pro-inflammatory mediators (Ungvari et al. 2013b). Endothelial senescence has also been recently implicated in the pathogenesis of cognitive impairment associated with DNA damage-mediated accelerated microvascular aging (e.g., radiation therapy–induced cognitive impairment (Ungvari et al. 2013b; Ungvari et al. 2017b)). There is growing evidence that senescent cells and their SASPs contribute to the pathogenesis of many other age-related diseases as well (Campisi 2013; Justice et al. 2018; Tchkonia and Kirkland 2018; Tchkonia et al. 2013; Campisi 2016; Chinta et al. 2014; Childs et al. 2016; Farr et al. 2017; Baker et al. 2011; Xu et al. 2018; Ogrodnik et al. 2018; Cohen and Torres 2019; Minamino et al. 2002). Indeed, depletion of cells
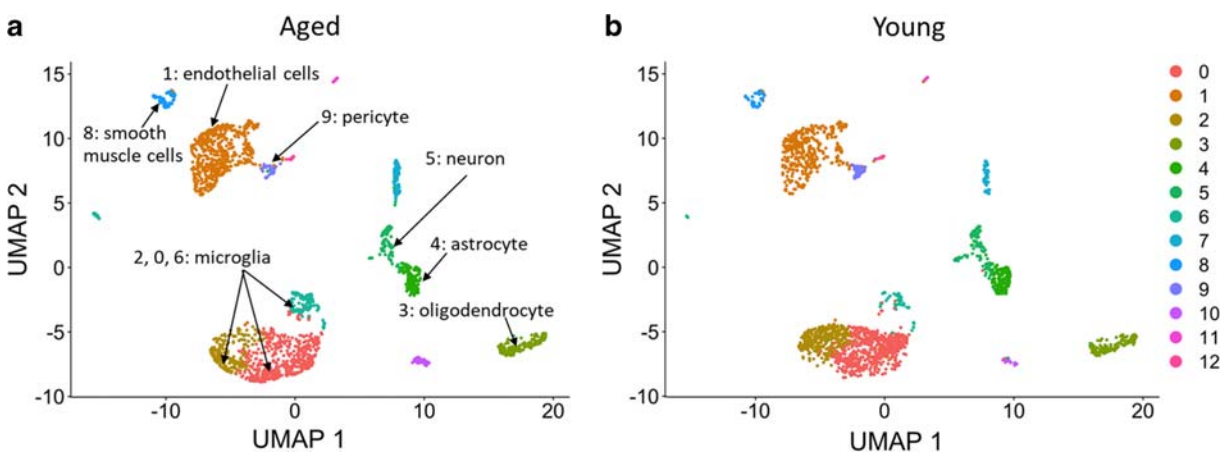

Fig. 1 Identification of cerebromicrovascular endothelial cells based on differentially expressed marker genes. Two-dimensional UMAP plots based on differentially expressed marker genes for $n = 4233$ cells, colored by cluster. Cluster identity was assigned based on previously reported differentially expressed genes listed in Table 1. Note that similar clusters were identified in samples derived from aged (panel **a**) and young (panel **b**) mouse brains
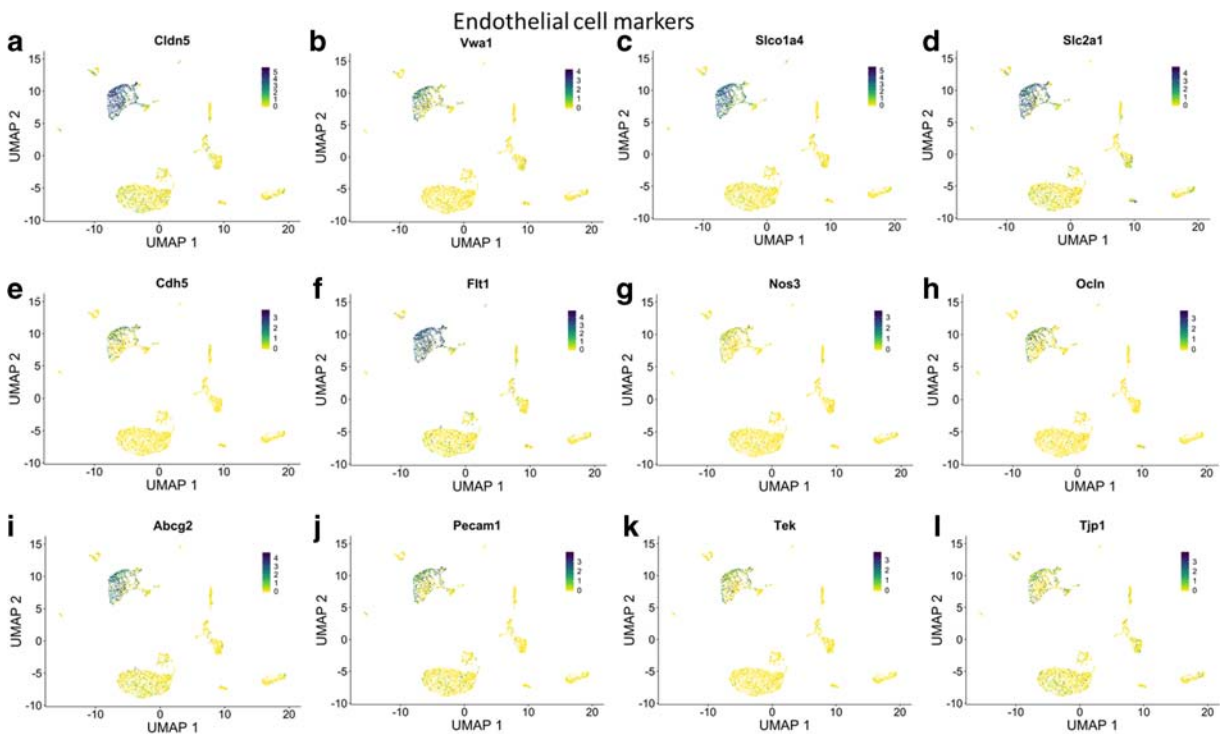
Fig. 2 Marker panel of canonical endothelial cell markers. Relative expression values for each cell in each cluster identified in the two-dimensional UMAP plots are shown. The canonical endothelial cell markers Cldn5, Slco1a4, Slc2a1, and Flt1 exhibit consistent labeling of cerebromicrovascular endothelial cells, while some other canonical endothelial cell markers (e.g., Nos3, Ocln) exhibit poor labeling of these cells using this methodology. NOTES: (Cldn5: claudin5, Wva1: Von Willebrand Factor A Domain Containing 1, Slco1a4: solute carrier organic anion transporter family member 1A4, Slc2a1: solute Carrier Family 2 Member 1, Cdh5: cadherin 5, Flt1: Vascular endothelial growth factor receptor 1, Nos3: endothelial nitric oxide synthase 3, Ocln: occludin, Abcg2: ATP-binding cassette super-family G member 2, Pecam1: Platelet endothelial cell adhesion molecule, Tek: Angiopoietin-1 receptor, Tjp1: Tight junction protein ZO-1

expressing the senescence marker cyclin-dependent kinase inhibitor p16INK4A in genetically modified mice prolongs median lifespan and improves overall health (Baker et al. 2016; Farr et al. 2017; Baker et al. 2011; Jeon et al. 2017; Abdul-Aziz et al. 2019; Kim et al. 2019; Patil et al. 2019; Xu et al. 2015; Roos et al. 2016; Baar et al. 2017), supporting a key role for cellular senescence in the process of aging. Strong evidence demonstrates that senolytic therapies exert significant endothelial protective effects in the aged brain and peripheral vasculature (Roos et al. 2016). Despite these advances, studies focusing on the mechanisms and consequences of endothelial senescence have been impeded by the lack of reliable methods to assess endothelial senescence burden in mouse models of VCI and AD. Evaluation of senescence-associated beta-galactosidase (SA-β-gal) is not enough to consistently detect senescent endothelial cells within the brain tissue. Antibodies to detect other senescence markers are notoriously non-specific. It is often very challenging to detect multiple senescence biomarkers within the same cells. Thus, there is a pressing need for novel methods for identification, quantification, and characterization of senescent cerebromicrovascular endothelial cells.

The present study was designed to develop a single-cell transcriptomics-based method to identify senescent cerebromicrovascular endothelial cells in the mouse brain. Over the past few years, powerful new methods have emerged for the investigation of single-cell transcriptomes. These technologies enable capture of mRNAs from single cells obtained from dissociated tissues, synthesis and amplification of cDNA, and generation of single-cell libraries for sequencing. We used a gel bead-in-emulsion–based droplet sequencing method, which is ideal for studying a large amount of brain cells in an unbiased manner. To detect senescent endothelial cells in the aging
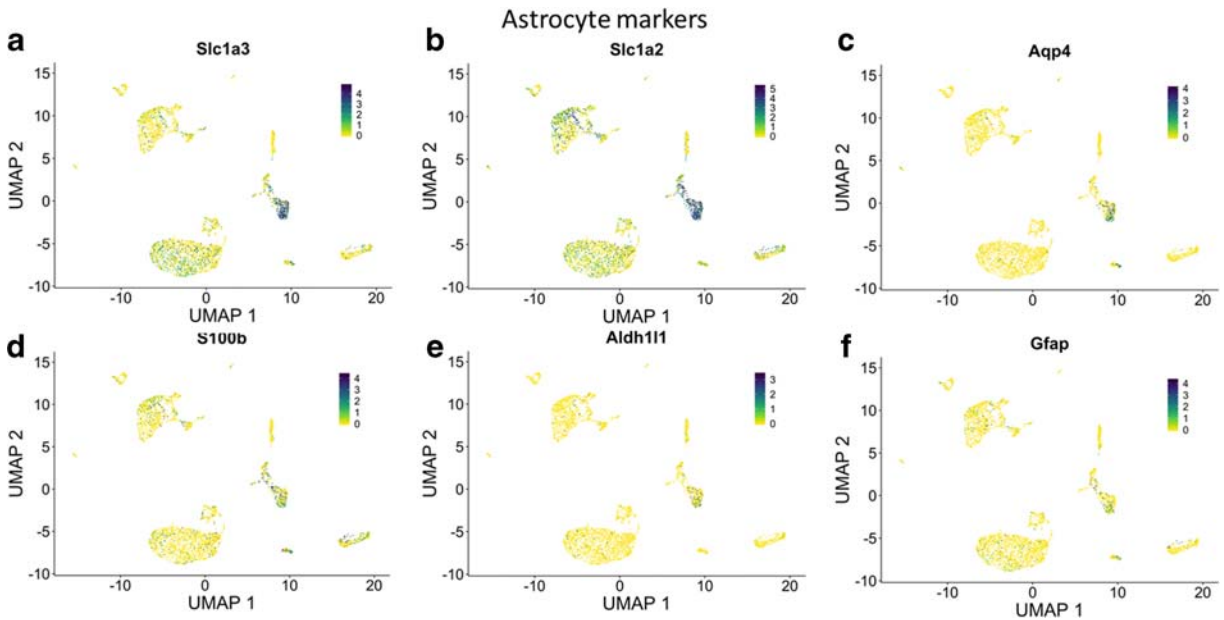
Fig. 3 Marker panel of canonical astrocyte markers. Relative expression values for each cell in each cluster identified in the two-dimensional UMAP plots are shown. Note that the canonical astrocyte markers Slc1a3 (sodium-dependent glutamate/aspartate transporter 1; GLAST1) and Slc1a2 (excitatory amino acid transporter 2; EAAT2) show strong labeling of astrocytes, whereas Aqp4 and Gfap exhibit poor labeling of these cells using this methodology. NOTES: Slc1a3: Excitatory amino acid transporter 1, Aqp4: Aquaporin 4, s100b: S100 Calcium Binding Protein B, Aldh1l1:aldehyde dehydrogenase 1 family member L1, Gfap: Glial fibrillary acidic protein

mouse brain, we analyzed cells in fractions enriched for cerebromicrovascular endothelial cells obtained from young (3-month-old) and aged (28-month-old) C57BL/6 mice. We identified cerebromicrovascular endothelial cells on the basis of their gene expression profile and matched transcriptomic signatures of cellular senescence to these cells.

Methods

Animals

Young (3-month-old, $n = 2$) and aged (28-month-old, $n = 4$) male C57BL/6 mice were purchased from the aging colony maintained by the National Institute on Aging at Charles River Laboratories (Wilmington, MA). The biological age of 28-month-old mice corresponds to that of $\sim$ 75-year-old humans. Mice were housed under specific pathogen-free barrier conditions in the Rodent Barrier Facility at University of Oklahoma Health Sciences Center under a controlled photoperiod (12-h light; 12-h dark) with unlimited access to water and were fed a standard AIN-93G diet (ad libitum). All procedures were approved by the Institutional Animal Use and Care Committees of the University of Oklahoma Health Sciences Center. All animal experiments complied with the ARRIVE guidelines and were carried out in accordance with the National Institutes of Health guide for the care and use of Laboratory animals (NIH Publications No. 8023, revised 1978).

Tissue processing, cell isolation

Brain tissue was harvested from two young and four aged mice (killed with CO_2) that had been exsanguinated by transcardial PBS perfusion (Tarantini et al. 2019b). The brains were quickly removed and rinsed in ice-cold PBS and minced into $\approx$ -mm^3 pieces. The tissue samples were washed twice in ice-cold 1X PBS by low-speed centrifugation (50 g, 3 min). The diced tissue was digested in a prewarmed buffer solution containing collagenase (800-U/g tissue), hyaluronidase (2.5-U/g tissue), and elastase (3-U/g tissue) in 1-mL PBS/100-mg tissue for 45 min at 37 °C in a rotating humid incubator. The digested tissue was passed through a 100-μm cell strainer. The single-cell lysate was centrifuged for 2 min at 70 g. After removing the supernatant, the pellet was washed twice in cold PBS supplemented with 2.5% fetal calf serum (FCS), and the
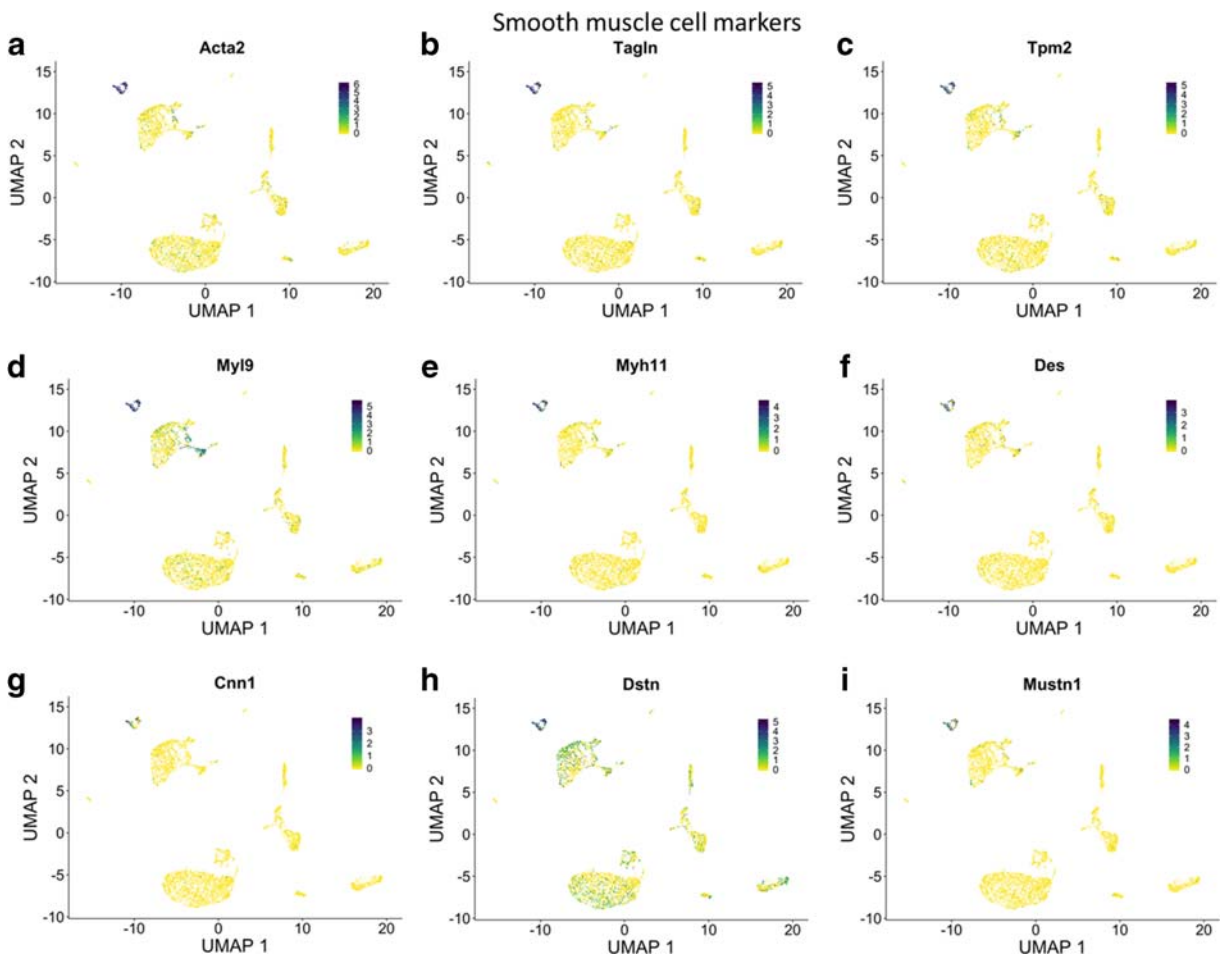
Smooth muscle cell markers

Fig. 4 Marker panel of canonical smooth muscle cell markers. Relative expression values for each cell in each cluster identified in the twodimensional UMAP plots are shown. NOTES: Acta2: Actin Alpha 2, Smooth Muscle, Tagln: Transgelin, Tpm2: β-Tropomyosin, myl9: Myosin regulatory light polypeptide 9, myh11: smooth muscle myosin heavy chain 11, Des: desmin, cnn1: Calponin 1, dstn: Destrin, mustn1: Musculoskeletal, Embryonic Nuclear Protein 1

suspension was centrifuged at 300g for 5 min at 4 °C. To obtain a fraction enriched for intact cerebromicrovascular endothelial cells and other cells associated with the neurovascular unit but depleted of neurons, the cell suspension was centrifuged using an OptiPrep gradient solution (Axi-Shield, PoC, Norway). Briefly, the cell pellet was resuspended in Hanks' balanced salt solution (HBSS) and mixed with 40% iodixanol thoroughly (final concentration 17% (v/v) iodixanol solution; ρ = 1.096 g/mL). Two milliliters of HBSS was layered on top and centrifuged at 400g for 15 min at 20 °C. Using this method, endothelial cells and microglia cells, which are of similar size and density, as well as a smaller mixed population of smooth muscle cells, pericytes, oligodendrocytes, and astrocytes, band at the interface between HBSS and the 17% iodixanol layer. Cells in this layer

were gently collected and suspended in ice-cold PBS containing 0.4% BSA. The advantage of this method is that it yields intact, high quality cells that are ideal for transcriptomic studies.

Single-cell RNA sequencing

All the samples were simultaneously isolated and processed through all steps to generate stable cDNA libraries. After dissociation, cells were diluted in ice-cold PBS containing 0.4% BSA at a density of 1897 ± 410 cells/ μL (viable cells 95.9 ± 0.7%). Cells were loaded into a Chromium Single Cell 3′ Chip (10x Genomics, Pleasanton, California) and processed following the manufacturer's instructions. Library construction was performed using the Chromium Single Cell 3′ Library & Gel Bead
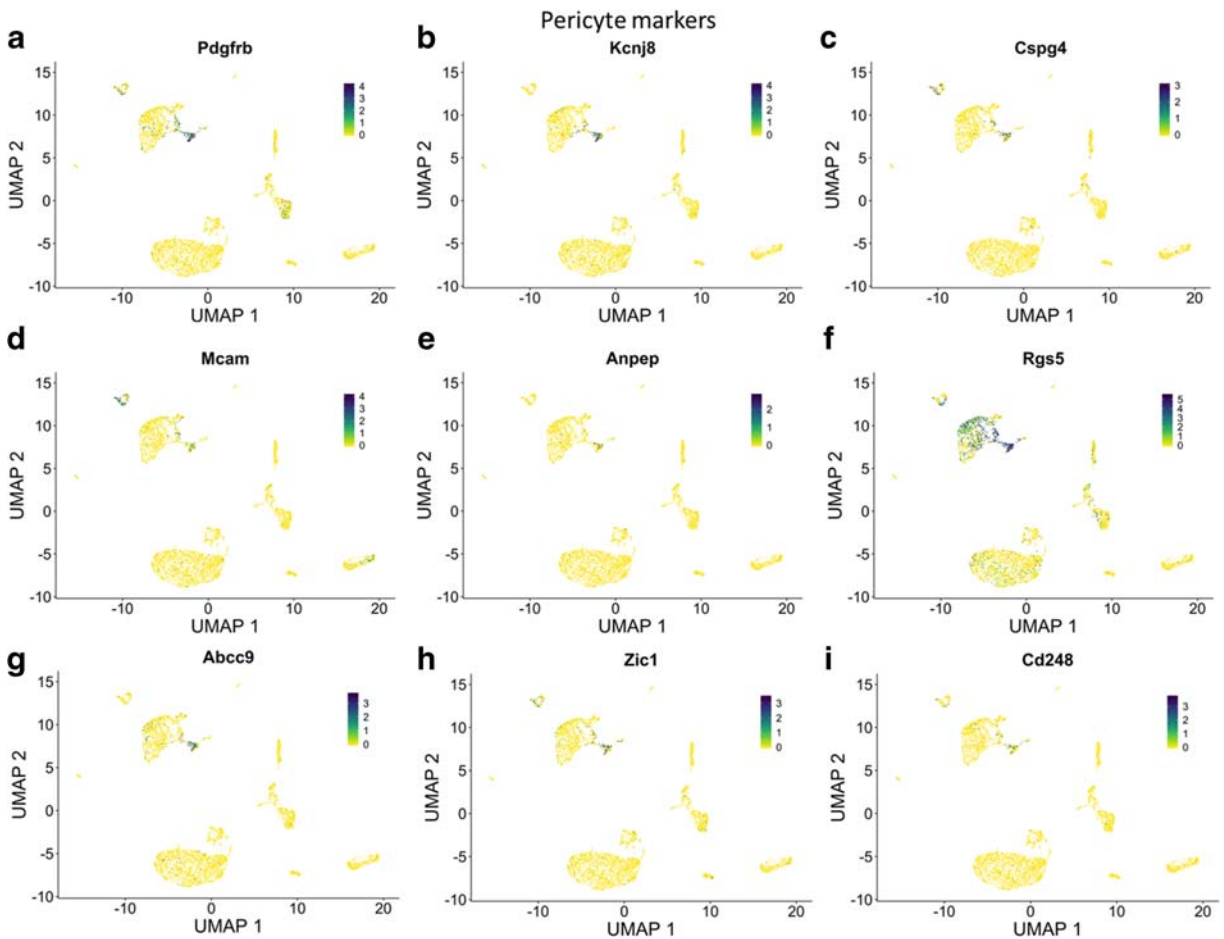
Fig. 5 Marker panel of canonical pericyte markers. Relative expression values for each cell in each cluster identified in the two-dimensional UMAP plots are shown. NOTES: pdgfrb: Platelet Derived Growth Factor Receptor Beta, kcnj8: Potassium Inwardly Rectifying Channel Subfamily J Member 8, cspg4: Chondroitin Sulfate Proteoglycan 4, mcam: Melanoma Cell Adhesion Molecule, anpep: Alanyl Aminopeptidase, rgs5: Regulator of G-protein signaling 5, abcc9: ATP Binding Cassette Subfamily C Member 9, zic1: Zic Family Member 1, cd248: Endosialin

Kit v2 (Catalog# 120267, lot# 152660; 10x Genomics, Pleasanton, California). Libraries were pooled based on their molar concentrations. Pooled library was sequenced on one high-output lane of the NovaSeq 6000 instrument (Illumina, San Diego, California). To de-multiplex samples, process barcodes, align and filter reads, and generate feature barcode matrices, we used 10x Genomics Cell Ranger (v3.0.2) pipeline (10x Genomics, Pleasanton, California) according to the manufacturer's instructions. Reads were mapped to the 10x Genomics reference of mm10 mouse transcriptome (v.1.2.0).

Analysis of single-cell datasets

The downstream analyses of Cell Ranger output were performed with the help of Seurat (v3.1) workflow implemented as an R package (R v3.6.0) (Stuart et al. 2019; Butler et al. 2018). Data obtained in each young and each aged samples were pooled. Our initial dataset contained 9091 cells, and the median number of genes per cell was 518. In the first step, low-quality cells were removed. Cells with extremely high or low number of unique genes and cells with extremely high percentage of reads that map to the mitochondrial genome were excluded from the further analysis (Ilicic et al. 2016; Luecken and Theis 2019). After this quality control step, the final dataset consisted of data from 4233 cells (2157 aged and 2076 young cells). We normalized the feature expression measurements using the *NormalizeData* function for each cell by the total expression, using the scale factor 10,000. The results were log-transformed
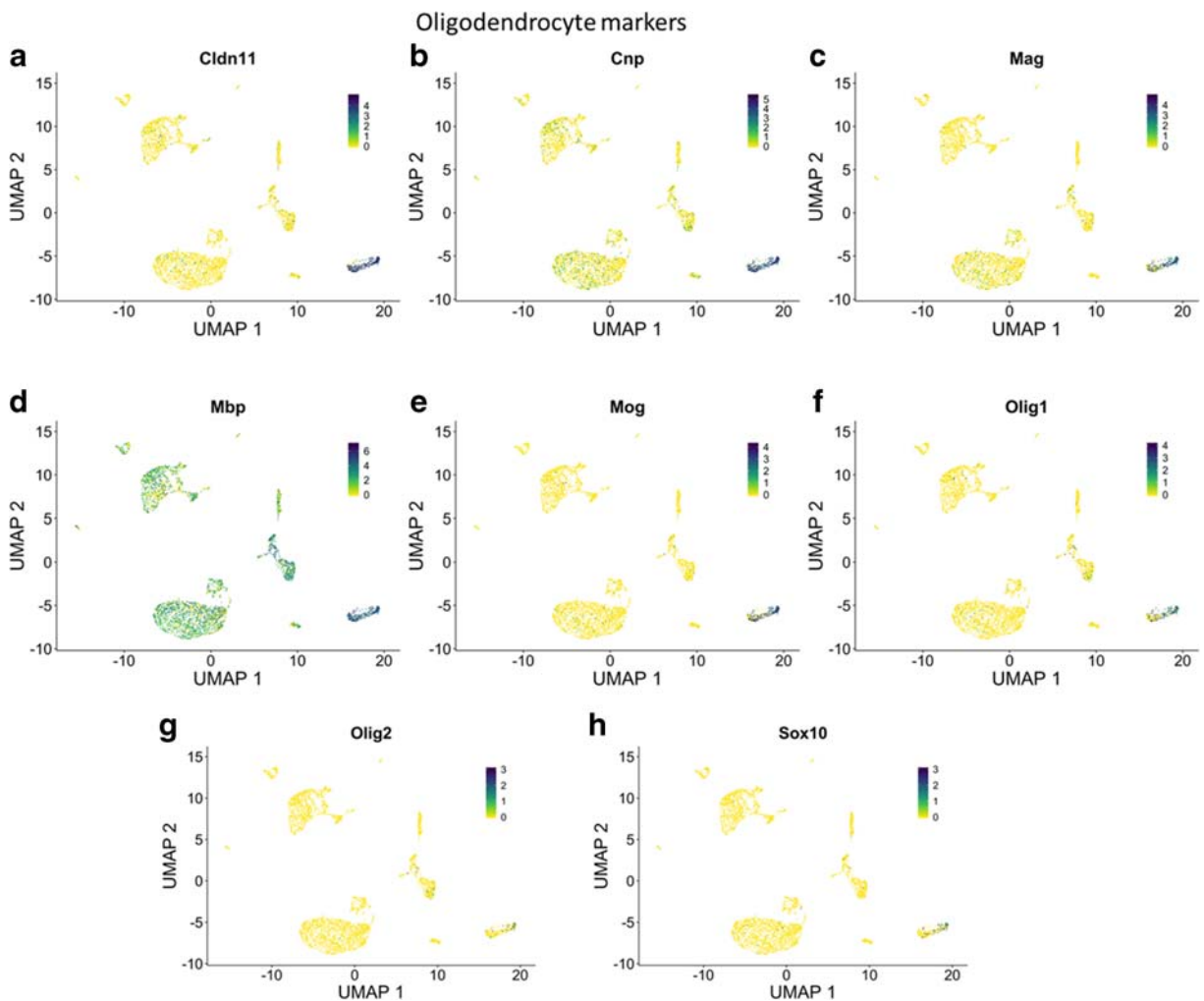
Fig. 6 Marker panel of canonical oligodendrocyte markers. Relative expression values for each cell in each cluster identified in the twodimensional UMAP plots are shown. NOTES: cnp: 2',3'-Cyclic Nucleotide 3' Phosphodiesterase, mag: Myelin Associated Glycoprotein, mbp: Myelin basic protein, mog: Myelin oligodendrocyte glycoprotein, olig1: Oligodendrocyte Transcription Factor 1, olig2: Oligodendrocyte Transcription Factor 2, sox10: Transcription factor SOX-10)

within the same step. Before the dimension reduction, the data was scaled by the *ScaleData* function.

The feature selection was performed with the help of the *FindVariableGenes* function. We identified 2000 genes which exhibit the highest cell-to-cell variation in the dataset (Brennecke et al. 2013). These variable features were used to run principal component analysis (PCA) on the data by the *RunPCA* function. The first 15 component of PCA was considered to cluster the cells. The cells were clustered with by the *FindClusters* function. We used the unbiased Louvain clustering algorithm with the resolution parameter 0.3 (arXiv:0803.0476 (physics.soc-ph) accessed at https://arxiv.org/abs/0803.0476) (Blondel et al. 2008).

Cluster-specific markers were identified by calculating differential gene expression between cells in the cluster versus all the other cells using the MAST (model-based analysis of single-cell transcriptomics) method (Finak et al. 2015). The MAST method was designed to handle the special challenged associated with singe-cell datasets, including the dropout events. The MAST method was implemented in the *MAST* (v1.12.0) R/Bioconductor package and called by Seurat (v3.1) workflow.

Visualization of our filtered, normalized, and scaled data was performed by uniform manifold approximation and projection algorithm (UMAP) implemented in the R package *uwot* (v0.1.4) and called by Seurat (v3.1)
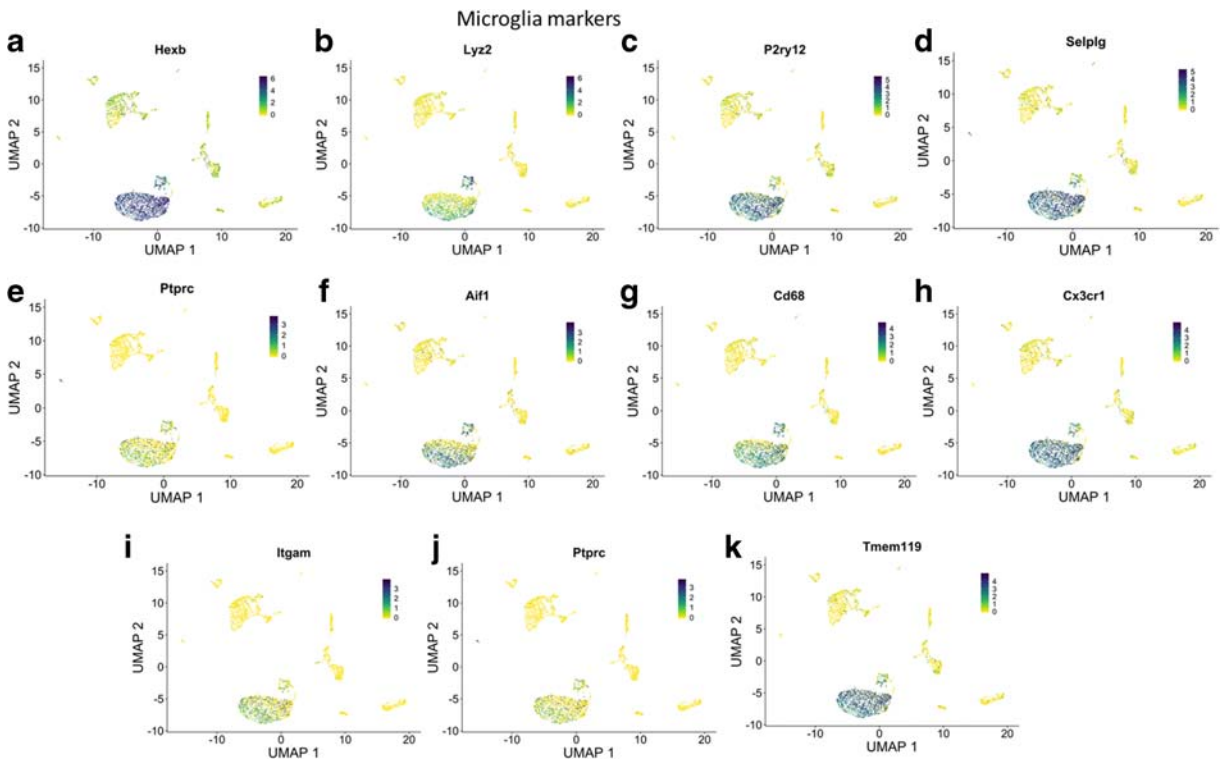
Fig. 7 Marker panel of canonical microglia markers. Relative expression values for each cell in each cluster identified in the twodimensional UMAP plots are shown. NOTES: (Cldn5: claudin5, Wva1: Von Willebrand Factor A Domain Containing 1, Slco1a4: solute carrier organic anion transporter family member 1A4, Slc2a1: solute Carrier Family 2 Member 1, Cdh5: cadherin 5, Flt1: Vascular endothelial growth factor receptor 1, Nos3: endo-thelial nitric oxide synthase 3, Ocln: occludin, Abcg2: ATP-binding cassette super-family G member 2, Pecam1: Platelet endothelial cell adhesion molecule, Tek: Angiopoietin-1 receptor, Tjp1: Tight junction protein ZO-1, Slc1a3: Excitatory amino acid transporter 1, Aqp4: Aquaporin 4, s100b: S100 Calcium Binding Protein B, Aldh1l1:aldehyde dehydrogenase 1 family member L1, Gfap: Glial fibrillary acidic protein, Acta2: Actin Alpha 2, Smooth Muscle, Tagln: Transgelin, Tpm2: β-Tropomyosin, myl9: Myosin regulatory light polypeptide 9, myh11: smooth muscle myosin heavy chain 11, Des: desmin, cnn1: Calponin 1, dstn: Destrin, mustn1: Musculoskeletal, Embryonic Nuclear Protein 1, pdgfrb: Platelet Derived Growth Factor Receptor Beta, kcnj8: Potassium Inwardly Rectifying Channel Subfamily J Member 8, cspg4: Chondroitin Sulfate Proteoglycan 4, mcam: Melanoma Cell Adhesion Molecule, anpep: Alanyl Aminopeptidase,rgs5: Regulator of G-protein signaling 5, abcc9: ATP Binding Cassette Subfamily C Member 9, zic1: Zic Family Member 1, cd248: Endosialin, cnp: 2′,3′-Cyclic Nucleotide 3′ Phosphodiesterase, mag: Myelin Associated Glycoprotein, mbp: Myelin basic protein, mog: Myelin oligodendrocyte glycoprotein,olig1: Oligodendrocyte Transcription Factor 1, olig2: Oligodendrocyte Transcription Factor 2, sox10: Transcription factor SOX-10)

workflow (arXiv:1802.03426 (stat.ML) accessed at https://arxiv.org/abs/1802.03426).

We realize that choice of data clustering method is dependent on the type of data. UMAP was chosen

Table 2 Senescence marker genes. *SASP*, senescence-associated secretory phenotype

| Gene category	Number of genes	Genes
Senescence core genes	10	Cdkn2a, Bmi1, Trp53, Hmga1, Chek1, Chek2, Prodh, Tnfrsf10b, Cdkn1a, Dao
Senescence effector genes	9	Ppp1ca, Ahcy, Brf1, Map 2 k3, Map 2 k6, Smurf2, Tgfb1i1, Srsf1, Angptl2
SASP genes	44	Ccl2, Ccl24, Ccl3, Ccl5, Ctnnb1, Cxcl1, Cxcl10, Cxcl12, Cxcl2, Cxcl16, Hgf, Hmgb1, Icam1, Igfbp2, Igfbp3, Igfbp4, Igfbp5, Igfbp6, Igfbp7, Il15, Il18, Il1a, Il1b, Il2, Il6, Mif, Mmp12, Mmp13, Mmp14, Pgf, Plat, Timp2, Serpine1, Ccl3, Ccl4, Ang, Csf2, Kitl, Serpine2, Tnfrsf1a, Hgf, Nrg1, Ereg, Areg
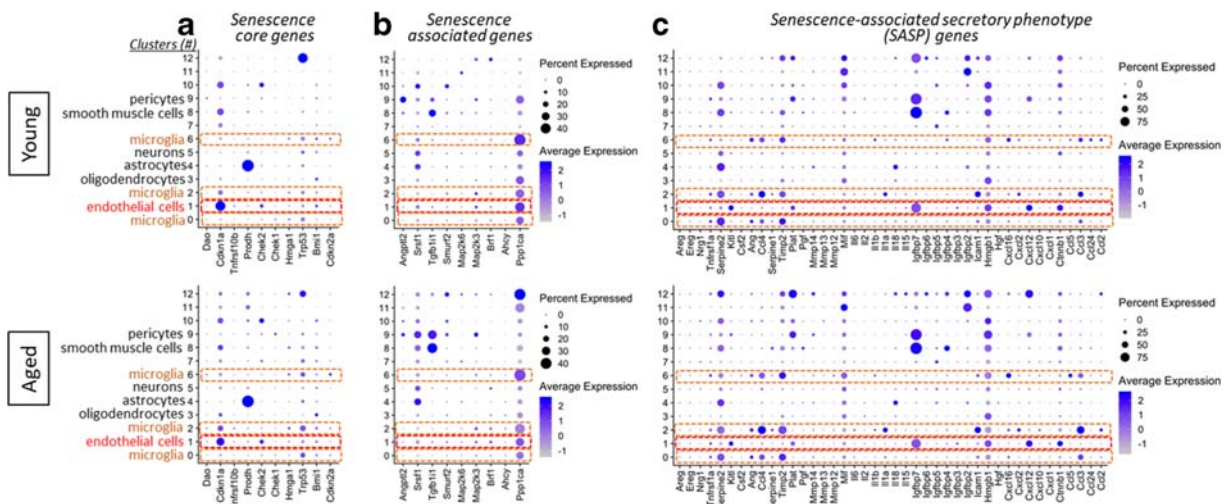
Fig. 8 Expression of senescence marker genes in different cell types in the young and aged mouse brain. Bubble plots show relative expression of senescence markers, including senescence core genes (panel A), senescence-associated effector genes (panel B), and genes that encode SASP factors (panel C), across clusters in young and aged mouse brains. Bubble size is proportional to percentage of cells expressing a gene, and color intensity is proportional to average-scaled gene expression within a cluster. Red fonts indicate cells constituting the neurovascular unit

instead of the more popular t-SNE (t-distributed stochastic neighborhood embedding) because it provided a better separation of the known cell types, as it was reported by Becht et al. (Becht et al. 2018) UMAP reduces high-dimensional data into two dimensions, which can be visualized in a scatter plot. All the plots were created by the built-in functions of Seurat (v3.1) workflow and the *ggplot* (v3.2.1) R/tidyverse package.

Assessment of the expression of senescence-related genes

Our goal was to identify senescent endothelial cells on the basis of their gene expression profile. To achieve that goal, senescence-related gene expression was characterized at the individual cell level by calculating a modified enrichment score (Subramanian et al. 2005) for each cell. In brief, for each cell, the expressed genes were ranked from the highest to the lowest abundance based on their scaled, normalized expression. A list of senescence-related core genes, effector genes, and genes encoding secreted proteins that constitute the SASP was compiled on the basis of the literature (Table 1) (Carnero 2013; Nagano et al. 2016). The target gene list for the enrichment score calculation contained each category of genes. The target gene list was assessed by iterating through the ranked gene list in each cell and adding a constant to the variable (called the running enrichment

score, RES) whenever the next gene on the ranked list is present among the target genes. If it is not present, the constant is subtracted from the RES. The largest deviation of the RES variable from 0 is considered the enrichment score of the given cell. If none of the target genes is expressed in the cell, then the enrichment score is set to 0. Positive numbers indicate accumulation of target genes among the upregulated genes.

Results

Identification of cell types

We report 4233 single-cell transcriptomes (2157 aged and 2076 young cells) with cluster-assigned identity, validated by quality control measures. Unbiased Louvain clustering of cells resolved 13 robust, transcriptionally distinct clusters of cells (resolution parameter 0.3; Fig. 1). Cell clusters were identified by the significant, cluster-specific markers calculated by the MAST method (Table 1). Using this method, we identified 1016 cells as endothelial cells and 1875 cells as microglia. Other cell types identified included smooth muscle cells, pericytes, astrocytes, oligodendrocytes, and a small number of neurons (Fig. 1). Cellular composition was similar in samples obtained from young and aged mice (Fig. 1).
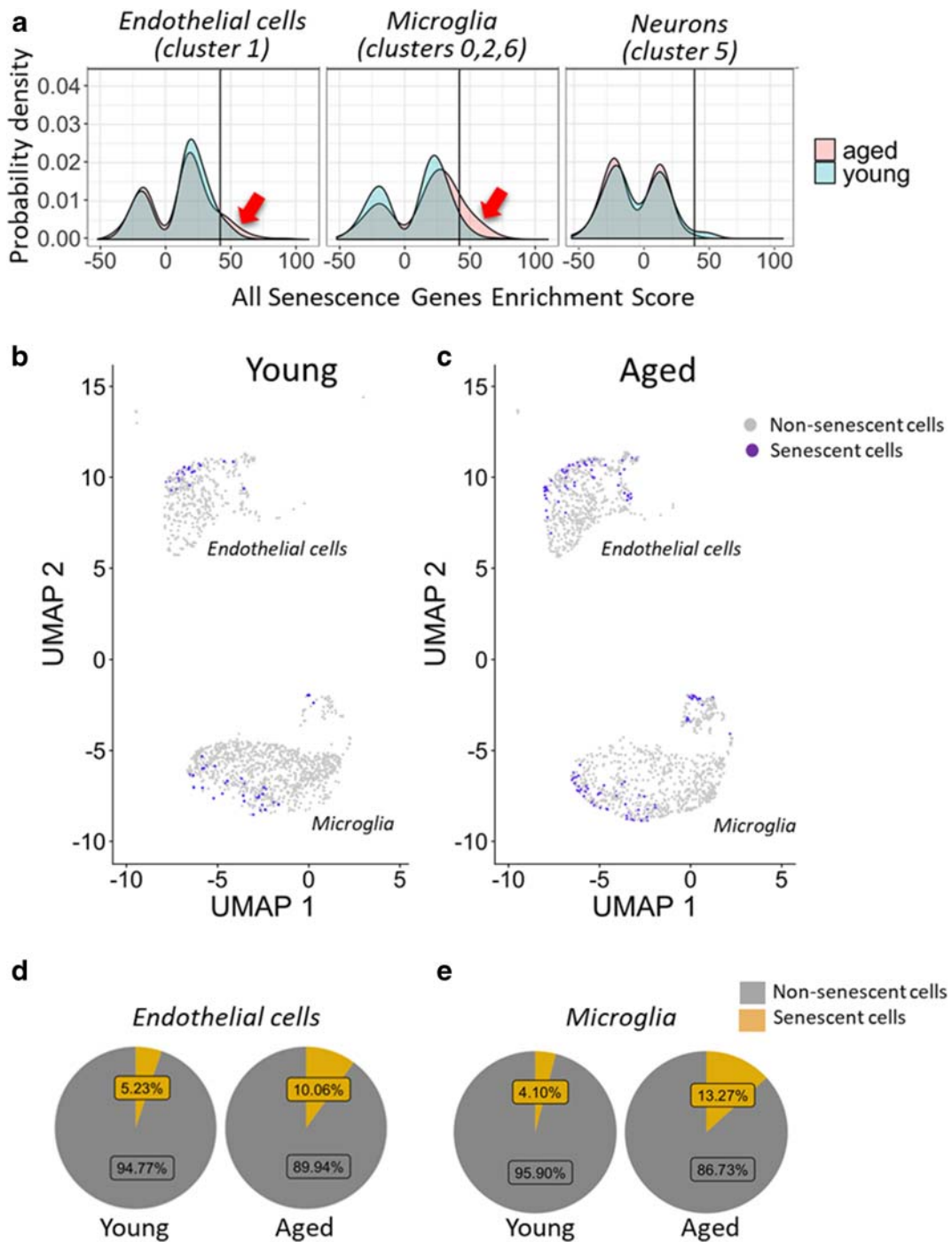
Fig. 9 Expression of senescence marker genes in different cell types in the young and aged mouse brain. Panel A Density-smoothed distribution for senescence gene enrichment scores (see "Methods") in endothelial cells (left), microglia (middle), and neuronal cells (right) in young and aged brains. Note that in aged brains compared with young brains, there is a more populous subgroup (arrows) of endothelial cells and microglia (but not neuronal cells) with high senescence gene enrichment scores (high

versus low expression defined relative to a score of 42; line). Panels B–C Cells with high expression of senescence markers (senescence score > 42) overlaid on UMAP plots for young (panel B) and aged brains (panel C). Panel D–E Pie charts showing percentage of endothelial cells (panel D) and microglia (panel E) with high expression of senescence markers in young and aged brains

Expression of canonical cell type markers

Our single-cell RNA sequencing (scRNA-seq) dataset provided a unique opportunity to investigate the expression of previously reported canonical cell type markers. Figures 2 to 7 depict cells expressing canonical endothelial cell (Fig. 2), smooth muscle cell (Fig. 3), pericyte (Fig. 4), astrocyte (Fig. 5), oligodendrocyte (Fig. 6), and microglia (Fig. 7) markers overlaid on UMAP plots of all cells.

Expression of senescence marker genes

A list of senescence marker genes (Table 2) was compiled on the basis of the available literature (Hernandez-Segura et al. 2017; Hernandez-Segura et al. 2018). Senescence marker genes include senescence core genes, senescence-associated effector genes, and genes that encode SASP factors. Mean expression across the panel of senescence markers was markedly different among the clusters (Fig. 8). This confirms that cell origin is a major determinant of heterogeneity of cellular senescence.

Quantitative analysis of senescent cells

To identify senescent subgroups of endothelial cells and other cell types, we first examined the expression of Cdkn2a and other commonly used senescence markers (Table 2). Because single-cell sequencing is inherently prone to dropout, or incomplete detection of genes expressed at low levels, we calculated a modified enrichment score for the whole senescence marker gene set for each cell as described in the "Methods." A major advantage of this method is that it considers both the expression amplitude of senescence-related genes and the number of senescence-related genes expressed in each cell. Figure 9A depicts density-smoothed distribution for senescence gene enrichment scores in endothelial cells, microglia, and neuronal cells derived from young and aged brains. We found that in aged brains, compared with young brains, there is a more populous subgroup of endothelial cells and microglia (but not neuronal cells), with high senescence gene enrichment scores. High versus low senescence gene enrichment scores were defined relative to a score of 42, on the basis of the shape of the distribution curves. We found that both endothelial cells and microglia with high expression of senescence markers are more prevalent in aged brains than in young samples (Fig. 9B–E).

Discussion

In this study, we applied single-cell RNA-seq technology to examine age-related endothelial senescence in the mouse brain. In doing so, we have identified a population of cerebromicrovascular endothelial cells with a unique transcriptional signature characteristic to cellular senescence. Our studies indicate that ~10% of cerebromicrovascular endothelial cells undergo cellular senescence in the mouse brain at a biological age that equals that of ~75-year-old humans. Importantly, similar prevalence of senescence endothelial cells was found in the aged mouse brain by independent methods (e.g., assessing senescent cells in aged p16-3MR senescence reporter mice; Csiszar and coworkers 2019, unpublished observation). The impact of senescence (Salminen et al. 2011) on the cerebromicrovascular endothelial phenotype and function is likely multifaceted, including dysregulation of cerebral blood flow and impairment of the blood-brain barrier and microcirculatory network architecture.

To our knowledge, our data provide the first transcriptional characterization of senescent cerebromicrovascular endothelial cells present in the aged mouse brain. As has been previously shown, we found overall low expression of senescence marker genes. While this study is not sufficient to distinguish unequivocally between cells in the presenescent-senescent continuum, it provides a useful method to compare senescent burden between groups. Notably, our method can also be adapted to evaluate efficiency of senolytic regimens (Childs et al. 2016; Xu et al. 2018; Jeon et al. 2017; Roos et al. 2016; Yabluchanksiy et al. 2020).

Because presenescent and senescent endothelial cells exhibit only relatively minor differences in expression of gene transcripts, studies using other cell-labeling techniques (e.g., cells from genetic senescence reporter mice expressing fluorescent protein tags (Jeon et al. 2017; Kim et al. 2019; Patil et al. 2019; Yabluchanksiy et al. 2020)) will likely be required to further optimize the senescence marker gene list used to calculate the enrichment score.

We propose that our single-cell RNA sequencing-based method can also be adapted to study the effect of aging on senescence in various brain cell types. As our data confirm that expression of senescent marker genes is highly cell type specific, we propose that a cell type–specific senescent marker gene set should be used to analyze each cluster separately. Due to their

pathophysiological relevance, single-cell RNA sequencing-based assessment of microglia senescence, astrocyte senescence (Tarantini et al. 2017a; Chinta et al. 2018; Cohen and Torres 2019; Salminen et al. 2011; Bhat et al. 2012; Bitto et al. 2010; Bussian et al. 2018; Gorg et al. 2018; Turnquist et al. 2019; Yamazaki et al. 2016), and pericyte senescence is of special interest.

References

Abdul-Aziz AM, Sun Y, Hellmich C, Marlein CR, Mistry J, Forde E, et al. Acute myeloid leukemia induces protumoral p16INK4a-driven senescence in the bone marrow microenvironment. Blood. 2019;133:446–56.

Baar MP, Brandt RMC, Putavet DA, Klein JDD, Derks KWJ, Bourgeois BRM, et al. Targeted apoptosis of senescent cells restores tissue homeostasis in response to chemotoxicity and aging. Cell. 2017;169:132–47 e16.

Baker DJ, Wijshake T, Tchkonia T, LeBrasseur NK, Childs BG, van de Sluis B, et al. Clearance of p16Ink4a-positive senescent cells delays ageing-associated disorders. Nature. 2011;479:232–6.

Baker DJ, Childs BG, Durik M, Wijers ME, Sieben CJ, Zhong J, et al. Naturally occurring p16(Ink4a)-positive cells shorten healthy lifespan. Nature. 2016;530:184–9.

Banki E, Sosnowska D, Tucsek Z, Gautam T, Toth P, Tarantini S, et al. Age-related decline of autocrine pituitary adenylate cyclase-activating polypeptide impairs angiogenic capacity

of rat cerebromicrovascular endothelial cells. J Gerontol A Biol Sci Med Sci. 2015;70:665–74.

Becht E, McInnes L, Healy J, Dutertre CA, Kwok IWH, Ng LG, et al. Dimensionality reduction for visualizing single-cell data using UMAP. Nat Biotechnol. 2018;37:38–44.

Bell RD, Zlokovic BV. Neurovascular mechanisms and blood-brain barrier disorder in Alzheimer's disease. Acta Neuropathol. 2009;118:103–13.

Bhat R, Crowe EP, Bitto A, Moh M, Katsetos CD, Garcia FU, et al. Astrocyte senescence as a component of Alzheimer's disease. PLoS One. 2012;7:e45069.

Bitto A, Sell C, Crowe E, Lorenzini A, Malaguti M, Hrelia S, et al. Stress-induced senescence in human and rodent astrocytes. Exp Cell Res. 2010;316:2961–8.

Blondel VD, Guillaume JL, Lambiotte R and Lefebvre E. Fast unfolding of communities in large networks. J Stat Mech-Theory Exp 2008.

Brennecke P, Anders S, Kim JK, Kolodziejczyk AA, Zhang X, Proserpio V, et al. Accounting for technical noise in single-cell RNA-seq experiments. Nat Methods. 2013;10:1093–5.

Brown WR, Thore CR. Review: cerebral microvascular pathology in ageing and neurodegeneration. Neuropathol Appl Neurobiol. 2011;37:56–74.

Bussian TJ, Aziz A, Meyer CF, Swenson BL, van Deursen JM, Baker DJ. Clearance of senescent glial cells prevents tau-dependent pathology and cognitive decline. Nature. 2018;562:578–82.

Butler A, Hoffman P, Smibert P, Papalexi E, Satija R. Integrating single-cell transcriptomic data across different conditions, technologies, and species. Nat Biotechnol. 2018;36:411–20.

Campisi J. Aging, cellular senescence, and cancer. Annu Rev Physiol. 2013;75:685–705.

Campisi J. Cellular senescence and lung function during aging. Yin and Yang. Ann Am Thorac Soc. 2016;13:S402–6.

Carnero A. Markers of cellular senescence. Methods Mol Biol. 2013;965:63–81.

Castillo-Carranza DL, Nilson AN, Van Skike CE, Jahrling JB, Patel K, Garach P, et al. Cerebral microvascular accumulation of tau oligomers in Alzheimer's disease and related tauopathies. Aging Dis. 2017;8:257–66.

Chen BR, Kozberg MG, Bouchard MB, Shaik MA, Hillman EM. A critical role for the vascular endothelium in functional neurovascular coupling in the brain. J Am Heart Assoc. 2014;3:e000787.

Childs BG, Baker DJ, Wijshake T, Conover CA, Campisi J, van Deursen JM. Senescent intimal foam cells are deleterious at all stages of atherosclerosis. Science. 2016;354:472–7.

Chinta SJ, Woods G, Rane A, Demaria M. Campisi J and Andersen JK. Exp Gerontol: Cellular senescence and the aging brain; 2014.

Chinta SJ, Woods G, Demaria M, Rane A, Zou Y, McQuade A, et al. Cellular senescence is induced by the environmental neurotoxin paraquat and contributes to neuropathology linked to Parkinson's disease. Cell Rep. 2018;22:930–40.

Cifuentes D, Poittevin M, Bonnin P, Ngkelo A, Kubis N, Merkulova-Rainon T, et al. Inactivation of nitric oxide synthesis exacerbates the development of Alzheimer disease pathology in APPPS1 mice (amyloid precursor protein/presenilin-1). Hypertension. 2017;70:613–23.

Clark LR, Berman SE, Rivera-Rivera LA, Hoscheidt SM, Darst BF, Engelman CD, et al. Macrovascular and microvascular

cerebral blood flow in adults at risk for Alzheimer's disease. Alzheimers Dement (Amst). 2017;7:48–55.

Cohen J, Torres C. Astrocyte senescence: evidence and significance. Aging Cell. 2019;18:e12937.

Csipo T, Fulop GA, Lipecz A, Tarantini S, Kiss T, Balasubramanian P, Csiszar A, Ungvari Z and Yabluchanskiy A. Short-term weight loss reverses obesity-induced microvascular endothelial dysfunction. Geroscience. 2018.

Csipo T, Lipecz A, Fulop GA, Hand RA, Ngo BN, Dzialendzik M, et al. Age-related decline in peripheral vascular health predicts cognitive impairment. Geroscience. 2019a;41:125–36.

Csipo T, Mukli P, Lipecz A, Tarantini S, Bahadli D, Abdulhussein O, et al. Assessment of age-related decline of neurovascular coupling responses by functional near-infrared spectroscopy (fNIRS) in humans. Geroscience. 2019b;41:495–509.

Csiszar A, Tarantini S, Fulop GA, Kiss T, Valcarcel-Ares MN, Galvan V, et al. Hypertension impairs neurovascular coupling and promotes microvascular injury: role in exacerbation of Alzheimer's disease. Geroscience. 2017.

Csiszar A, Yabluchanskiy A, Ungvari A, Ungvari Z, Tarantini S. Overexpression of catalase targeted to mitochondria improves neurovascular coupling responses in aged mice. Geroscience. 2019;41:609–17.

Farias Quipildor GE, Mao K, Hu Z, Novaj A, Cui MH, Gulinello M, et al. Central IGF-1 protects against features of cognitive and sensorimotor decline with aging in male mice. Geroscience. 2019;41:185–208.

Farr JN, Xu M, Weivoda MM, Monroe DG, Fraser DG, Onken JL, et al. Targeting cellular senescence prevents age-related bone loss in mice. Nat Med. 2017;23:1072–9.

Finak G, McDavid A, Yajima M, Deng J, Gersuk V, Shalek AK, et al. MAST: a flexible statistical framework for assessing transcriptional changes and characterizing heterogeneity in single-cell RNA sequencing data. Genome Biol. 2015;16:278.

Freeze WM, Bacskai BJ, Frosch MP, Jacobs HIL, Backes WH, Greenberg SM, et al. Blood-brain barrier leakage and microvascular lesions in cerebral amyloid angiopathy. Stroke. 2019;50:328–35.

Fulop GA, Kiss T, Tarantini S, Balasubramanian P, Yabluchanskiy A, Farkas E, et al. Nrf2 deficiency in aged mice exacerbates cellular senescence promoting cerebrovascular inflammation. Geroscience. 2018;40:513–21.

Fulop GA, Ahire C, Csipo T, Tarantini S, Kiss T, Balasubramanian P, et al. Cerebral venous congestion promotes blood-brain barrier disruption and neuroinflammation, impairing cognitive function in mice. Geroscience. 2019a;41:575–89.

Fulop GA, Tarantini S, Yabluchanskiy A, Molnar A, Prodan CI, Kiss T, et al. Role of age-related alterations of the cerebral venous circulation in the pathogenesis of vascular cognitive impairment. Am J Physiol Heart Circ Physiol. 2019b;316: H1124–40.

Gorg B, Karababa A, Haussinger D. Hepatic encephalopathy and astrocyte senescence. J Clin Exp Hepatol. 2018;8:294–300.

Hase Y, Polvikoski TM, Firbank MJ, Craggs LJL, Hawthorne E, Platten C, et al. Small vessel disease pathological changes in neurodegenerative and vascular dementias concomitant with autonomic dysfunction. Brain Pathol. 2020;30:191–202.

Hernandez-Segura A, de Jong TV, Melov S, Guryev V, Campisi J, Demaria M. Unmasking transcriptional heterogeneity in senescent cells. Curr Biol. 2017;27:2652–60 e4.

Hernandez-Segura A, Nehme J, Demaria M. Hallmarks of cellular senescence. Trends Cell Biol. 2018;28:436–53.

Ilicic T, Kim JK, Kolodziejczyk AA, Bagger FO, McCarthy DJ, Marioni JC, et al. Classification of low quality cells from single-cell RNA-seq data. Genome Biol. 2016;17:29.

Jeon OH, Kim C, Laberge RM, Demaria M, Rathod S, Vasserot AP, et al. Local clearance of senescent cells attenuates the development of post-traumatic osteoarthritis and creates a pro-regenerative environment. Nat Med. 2017;23:775–81.

Justice JN, Gregory H, Tchkonia T, LeBrasseur NK, Kirkland JL, Kritchevsky SB, et al. Cellular senescence biomarker p16INK4a+ cell burden in thigh adipose is associated with poor physical function in older women. J Gerontol A Biol Sci Med Sci. 2018;73:939–45.

Khosla S, Farr JN, Kirkland JL. Inhibiting cellular senescence: a new therapeutic paradigm for age-related osteoporosis. J Clin Endocrinol Metab. 2018;103:1282–90.

Kim HN, Chang J, Iyer S, Han L, Campisi J, Manolagas SC, et al. Elimination of senescent osteoclast progenitors has no effect on the age-associated loss of bone mass in mice. Aging Cell. 2019;18:e12923.

Kirkland JL, Tchkonia T. Cellular senescence: a translational perspective. EBioMedicine. 2017;21:21–8.

Kisler K, Nelson AR, Montagne A, Zlokovic BV. Cerebral blood flow regulation and neurovascular dysfunction in Alzheimer disease. Nat Rev Neurosci. 2017;18:419–34.

Kiss T, Balasubramanian P, Valcarcel-Ares MN, Tarantini S, Yabluchanskiy A, Csipo T, et al. Nicotinamide mononucleotide (NMN) treatment attenuates oxidative stress and rescues angiogenic capacity in aged cerebromicrovascular endothelial cells: a potential mechanism for prevention of vascular cognitive impairment. GeroScience. 2019a;41:619–30 in press.

Kiss T, Giles CB, Tarantini S, Yabluchanskiy A, Balasubramanian P, Gautam T, et al. Nicotinamide mononucleotide (NMN) supplementation promotes anti-aging miRNA expression profile in the aorta of aged mice, predicting epigenetic rejuvenation and anti-atherogenic effects. Geroscience. 2019b;41(4):419–39.

LeBrasseur NK, Tchkonia T, Kirkland JL. Cellular senescence and the biology of aging, disease, and frailty. Nestle Nutr Inst Workshop Ser. 2015;83:11–8.

Lin AL, Zheng W, Halloran JJ, Burbank RR, Hussong SA, Hart MJ, et al. Chronic rapamycin restores brain vascular integrity and function through NO synthase activation and improves memory in symptomatic mice modeling Alzheimer's disease. J Cereb Blood Flow Metab. 2013;33:1412–21.

Lipecz A, Csipo T, Tarantini S, Hand RA, Ngo BN, Conley S, et al. Age-related impairment of neurovascular coupling responses: a dynamic vessel analysis (DVA)-based approach to measure decreased flicker light stimulus-induced retinal arteriolar dilation in healthy older adults. Geroscience. 2019;41(3):341–9.

Luecken MD, Theis FJ. Current best practices in single-cell RNA-seq analysis: a tutorial. Mol Syst Biol. 2019;15:e8746.

Mackic JB, Weiss MH, Miao W, Kirkman E, Ghiso J, Calero M, et al. Cerebrovascular accumulation and increased blood-brain barrier permeability to circulating Alzheimer's amyloid beta peptide in aged squirrel monkey with cerebral amyloid angiopathy. J Neurochem. 1998;70:210–5.

Minamino T, Miyauchi H, Yoshida T, Ishida Y, Yoshida H, Komuro I. Endothelial cell senescence in human

atherosclerosis: role of telomere in endothelial dysfunction. Circulation. 2002;105:1541–4.

Montagne A, Barnes SR, Sweeney MD, Halliday MR, Sagare AP, Zhao Z, et al. Blood-brain barrier breakdown in the aging human hippocampus. Neuron. 2015;85:296–302.

Montagne A, Zhao Z, Zlokovic BV. Alzheimer's disease: a matter of blood-brain barrier dysfunction? J Exp Med. 2017;214: 3151–69.

Nagano T, Nakano M, Nakashima A, Onishi K, Yamao S, Enari M, et al. Identification of cellular senescence-specific genes by comparative transcriptomics. Sci Rep. 2016;6:31758.

Nagyoszi P, Nyul-Toth A, Fazakas C, Wilhelm I, Kozma M, Molnar J, et al. Regulation of NOD-like receptors and inflammasome activation in cerebral endothelial cells. J Neurochem. 2015;135:551–64.

Nelson AR, Sweeney MD, Sagare AP, Zlokovic BV. Neurovascular dysfunction and neurodegeneration in dementia and Alzheimer's disease. Biochim Biophys Acta. 1862;2016:887–900.

Nelson AR, Sagare AP, Zlokovic BV. Role of clusterin in the brain vascular clearance of amyloid-beta. Proc Natl Acad Sci U S A. 2017;114:8681–2.

Nielsen RB, Egefjord L, Angleys H, Mouridsen K, Gejl M, Moller A, et al. Capillary dysfunction is associated with symptom severity and neurodegeneration in Alzheimer's disease. Alzheimers Dement. 2017;13:1143–53.

Ogrodnik M, Zhu Y, Langhi LGP, Tchkonia T, Kruger P, Fielder E, et al. Obesity-induced cellular senescence drives anxiety and impairs neurogenesis. Cell Metab. 2018;29:1061–1077.e8.

Patil P, Dong Q, Wang D, Chang J, Wiley C, Demaria M, et al. Systemic clearance of p16(INK4a)-positive senescent cells mitigates age-associated intervertebral disc degeneration. Aging Cell. 2019;18:e12927.

Petzold GC, Murthy VN. Role of astrocytes in neurovascular coupling. Neuron. 2011;71:782–97.

Roos CM, Zhang B, Palmer AK, Ogrodnik MB, Pirtskhalava T, Thalji NM, et al. Chronic senolytic treatment alleviates established vasomotor dysfunction in aged or atherosclerotic mice. Aging Cell. 2016;15:973–7.

Sagare AP, Bell RD, Zlokovic BV. Neurovascular defects and faulty amyloid-beta vascular clearance in Alzheimer's disease. J Alzheimers Dis. 2013;33(Suppl 1):S87–100.

Salminen A, Ojala J, Kaarniranta K, Haapasalo A, Hiltunen M, Soininen H. Astrocytes in the aging brain express characteristics of senescence-associated secretory phenotype. Eur J Neurosci. 2011;34:3–11.

Sen A, Hongpaisan J. Hippocampal microvasculature changes in association with oxidative stress in Alzheimer's disease. Free Radic Biol Med. 2018;120:192–203.

Shi Q, Hubbard GB, Kushwaha RS, Rainwater D, Thomas CA 3rd, Leland MM, et al. Endothelial senescence after high-cholesterol, high-fat diet challenge in baboons. Am J Physiol Heart Circ Physiol. 2007;292:H2913–20.

Silva GC, Abbas M, Khemais-Benkhiat S, Burban M, Ribeiro TP, Toti F, et al. Replicative senescence promotes prothrombotic responses in endothelial cells: role of NADPH oxidase- and cyclooxygenase-derived oxidative stress. Exp Gerontol. 2017;93:7–15.

Stanimirovic DB, Friedman A. Pathophysiology of the neurovascular unit: disease cause or consequence? J Cereb Blood Flow Metab. 2012;32:1207–21.

Stobart JL, Lu L, Anderson HD, Mori H, Anderson CM. Astrocyte-induced cortical vasodilation is mediated by D-serine and endothelial nitric oxide synthase. Proc Natl Acad Sci U S A. 2013;110:3149–54.

Stuart T, Butler A, Hoffman P, Hafemeister C, Papalexi E, Mauck WM 3rd, et al. Comprehensive integration of single-cell data. Cell. 2019;177:1888–902 e21.

Subramanian A, Tamayo P, Mootha VK, Mukherjee S, Ebert BL, Gillette MA, et al. Gene set enrichment analysis: a knowledge-based approach for interpreting genome-wide expression profiles. Proc Natl Acad Sci U S A. 2005;102: 15545–50.

Sweeney MD, Sagare AP, Zlokovic BV. Blood-brain barrier breakdown in Alzheimer disease and other neurodegenerative disorders. Nat Rev Neurol. 2018a;14:133–50.

Sweeney MD, Kisler K, Montagne A, Toga AW, Zlokovic BV. The role of brain vasculature in neurodegenerative disorders. Nat Neurosci. 2018b;21:1318–31.

Tarantini S, Tucsek Z, Valcarcel-Ares M, Toth P, Gautam T, Giles C, et al. Circulating IGF-1 deficiency exacerbates hypertension-induced microvascular rarefaction in the mouse hippocampus and retrosplenial cortex: implications for cerebromicrovascular and brain aging. Age (Dordr). 2016;38:273–89.

Tarantini S, Tran CHT, Gordon GR, Ungvari Z, Csiszar A. Impaired neurovascular coupling in aging and Alzheimer's disease: contribution of astrocyte dysfunction and endothelial impairment to cognitive decline. Exp Gerontol. 2017a;94:52–8.

Tarantini S, Valcarcel-Ares NM, Yabluchanskiy A, Springo Z, Fulop GA, Ashpole N, et al. Insulin-like growth factor 1 deficiency exacerbates hypertension-induced cerebral microhemorrhages in mice, mimicking the aging phenotype. Aging Cell. 2017b;16:469–79.

Tarantini S, Fulop GA, Kiss T, Farkas E, Zolei-Szenasi D, Galvan V, et al. Demonstration of impaired neurovascular coupling responses in TG2576 mouse model of Alzheimer's disease using functional laser speckle contrast imaging. Geroscience. 2017c;39:465–73.

Tarantini S, Yabluchanksiy A, Fulop GA, Hertelendy P, Valcarcel-Ares MN, Kiss T, et al. Pharmacologically induced impairment of neurovascular coupling responses alters gait coordination in mice. Geroscience. 2017d;39:601–14.

Tarantini S, Valcarcel-Ares MN, Yabluchanskiy A, Tucsek Z, Hertelendy P, Kiss T, et al. Nrf2 deficiency exacerbates obesity-induced oxidative stress, neurovascular dysfunction, blood brain barrier disruption, neuroinflammation, amyloidogenic gene expression and cognitive decline in mice, mimicking the aging phenotype. J Gerontol A Biol Sci Med Sci. 2018;7:853–63 in press.

Tarantini S, Yabluchanskiy A, Csipo T, Fulop G, Kiss T, Balasubramanian P, et al. Treatment with the poly (ADP-ribose) polymerase inhibitor PJ-34 improves cerebromicrovascular endothelial function, neurovascular coupling responses and cognitive performance in aged mice, supporting the NAD+ depletion hypothesis of neurovascular aging. Geroscience. 2019a.

Tarantini S, Valcarcel-Ares MN, Toth P, Yabluchanskiy A, Tucsek Z, Kiss T, et al. Nicotinamide mononucleotide (NMN) supplementation rescues cerebromicrovascular endothelial function and neurovascular coupling responses and improves cognitive function in aged mice. Redox Biol. 2019b;24:101192.

Tchkonia T, Kirkland JL. Aging, cell senescence, and chronic disease: emerging therapeutic strategies. JAMA. 2018;320: 1319–20.

Tchkonia T, Morbeck DE, Von Zglinicki T, Van Deursen J, Lustgarten J, Scrable H, et al. Fat tissue, aging, and cellular senescence. Aging Cell. 2010;9:667–84.

Tchkonia T, Zhu Y, van Deursen J, Campisi J, Kirkland JL. Cellular senescence and the senescent secretory phenotype: therapeutic opportunities. J Clin Invest. 2013;123:966–72.

Toth P, Tucsek Z, Sosnowska D, Gautam T, Mitschelen M, Tarantini S, et al. Age-related autoregulatory dysfunction and cerebromicrovascular injury in mice with angiotensin II-induced hypertension. J Cereb Blood Flow Metab. 2013;33:1732–42.

Toth P, Tucsek Z, Tarantini S, Sosnowska D, Gautam T, Mitschelen M, et al. IGF-1 deficiency impairs cerebral myogenic autoregulation in hypertensive mice. J Cereb Blood Flow Metab. 2014;34:1887–97.

Toth P, Tarantini S, Springo Z, Tucsek Z, Gautam T, Giles CB, et al. Aging exacerbates hypertension-induced cerebral microhemorrhages in mice: role of resveratrol treatment in vasoprotection. Aging Cell. 2015;14:400–8.

Toth P, Tarantini S, Csiszar A, Ungvari Z. Functional vascular contributions to cognitive impairment and dementia: mechanisms and consequences of cerebral autoregulatory dysfunction, endothelial impairment, and neurovascular uncoupling in aging. Am J Physiol Heart Circ Physiol. 2017;312:H1–H20.

Tucsek Z, Toth P, Tarantini S, Sosnowska D, Gautam T, Warrington JP, et al. Aging exacerbates obesity-induced cerebromicrovascular rarefaction, neurovascular uncoupling, and cognitive decline in mice. J Gerontol A Biol Sci Med Sci. 2014a;69:1339–52.

Tucsek Z, Toth P, Sosnowsk D, Gautam T, Mitschelen M, Koller A, et al. Obesity in aging exacerbates blood brain barrier disruption, neuroinflammation and oxidative stress in the mouse hippocampus: effects on expression of genes involved in beta-amyloid generation and Alzheimer's disease. J Gerontol A Biol Sci Med Sci. 2014b;69:1212–26.

Turnquist C, Beck JA, Horikawa I, Obiorah IE, Von Muhlinen N, Vojtesek B, et al. Radiation-induced astrocyte senescence is rescued by Delta133p53. Neuro-Oncology. 2019;21:474–85.

Ungvari Z, Tucsek Z, Sosnowska D, Toth P, Gautam T, Podlutsky A, et al. Aging-induced dysregulation of Dicer1-dependent microRNA expression impairs angiogenic capacity of rat cerebromicrovascular endothelial cells. J Gerontol A Biol Sci Med Sci. 2013a;68:877–91.

Ungvari Z, Podlutsky A, Sosnowska D, Tucsek Z, Toth P, Deak F, et al. Ionizing radiation promotes the acquisition of a senescence-associated secretory phenotype and impairs angiogenic capacity in cerebromicrovascular endothelial cells: role of increased DNA damage and decreased DNA repair capacity in microvascular radiosensitivity. J Gerontol A Biol Sci Med Sci. 2013b;68:1443–57.

Ungvari Z, Tarantini S, Kirkpatrick AC, Csiszar A, Prodan CI. Cerebral microhemorrhages: mechanisms, consequences, and prevention. Am J Physiol Heart Circ Physiol. 2017a;312:H1128–43.

Ungvari Z, Tarantini S, Hertelendy P, Valcarcel-Ares MN, Fulop GA, Logan S, et al. Cerebromicrovascular dysfunction predicts cognitive decline and gait abnormalities in a mouse model of whole brain irradiation-induced accelerated brain senescence. Geroscience. 2017b;39:33–42.

Ungvari Z, Tarantini S, Kiss T, Wren JD, Giles CB, Griffin CT, et al. Endothelial dysfunction and angiogenesis impairment in the ageing vasculature. Nat Rev Cardiol. 2018a;15:555–65.

Ungvari Z, Tarantini S, Donato AJ, Galvan V, Csiszar A. Mechanisms of vascular aging. Circ Res. 2018b;123:849–67.

Van Skike CE, Jahrling JB, Olson AB, Sayre NL, Hussong SA, Ungvari Z, et al. Inhibition of mTOR protects the blood-brain barrier in models of Alzheimer's disease and vascular cognitive impairment. Am J Physiol Heart Circ Physiol. 2018;314: H693–703.

van Veluw SJ, Scherlek AA, Freeze WM, Ter Telgte A, van der Kouwe AJ, Bacskai BJ, et al. Different microvascular alterations underlie microbleeds and microinfarcts. Ann Neurol. 2019;86:279–92.

Voghel G, Thorin-Trescases N, Farhat N, Nguyen A, Villeneuve L, Mamarbachi AM, et al. Cellular senescence in endothelial cells from atherosclerotic patients is accelerated by oxidative stress associated with cardiovascular risk factors. Mech Ageing Dev. 2007;128:662–71.

Warrington JP, Ashpole N, Csiszar A, Lee YW, Ungvari Z, Sonntag WE. Whole brain radiation-induced vascular cognitive impairment: mechanisms and implications. J Vasc Res. 2013;50:445–57.

Wells JA, Christie IN, Hosford PS, Huckstepp RT, Angelova PR, Vihko P, et al. A critical role for purinergic signalling in the mechanisms underlying generation of BOLD fMRI responses. J Neurosci. 2015;35:5284–92.

Wilhelm I, Nyul-Toth A, Kozma M, Farkas AE, Krizbai IA. Role of pattern recognition receptors of the neurovascular unit in inflamm-aging. Am J Physiol Heart Circ Physiol. 2017;313: H1000–12.

Xu M, Palmer AK, Ding H, Weivoda MM, Pirtskhalava T, White TA, et al. Targeting senescent cells enhances adipogenesis and metabolic function in old age. Elife. 2015;4.

Xu M, Pirtskhalava T, Farr JN, Weigand BM, Palmer AK, Weivoda MM, et al. Senolytics improve physical function and increase lifespan in old age. Nat Med. 2018;24:1246–56.

Yabluchanksiy A, Tarantini S, Balasubramaniam P, Kiss T, Csipo T, Fulop GA, Lipecz A, del Favero J, Nyul-Toth A, Sonntag WE, Schwartzman ML, Campisi J, Csiszar A and Ungvari Z. Pharmacological or genetic depletion of senescent astrocytes prevents whole brain irradiation-induced impairment of neurovascular coupling responses protecting cognitive function in mice. Geroscience. 2020. in press.

Yamazaki Y, Baker DJ, Tachibana M, Liu CC, van Deursen JM, Brott TG, et al. Vascular cell senescence contributes to blood-brain barrier breakdown. Stroke. 2016;47:1068–77.

Zlokovic BV. The blood-brain barrier in health and chronic neurodegenerative disorders. Neuron. 2008;57:178–201.